Research Article

International Journal of Distributed Sensor Networks

International Journal of Distributed Sensor Networks
2016, Vol. 12(9)

DOI: 10.1177/1550147716668063
ijdsn.sagepub.com
SAGE

Design and performance analysis of wireless body area networks in complex indoor e-Health hospital environments for patient remote monitoring

Erik Aguirre[1], Peio Lopez-Iturri[1], Leyre Azpilicueta[2], Carmen Rivarés[1], José Javier Astrain[3], Jesús Villadangos[3] and Francisco Falcone[1]

Abstract

In this article, the design and performance analysis of wireless body area network–based systems for the transmission of medical information readable in an android-based application deployed within complex indoor e-Health scenarios is presented. The scenario under analysis is an emergency room area, where a patient is being monitored remotely with the aid of wearable wireless sensors placed at different body locations. Due to the advent of Internet of Things, in the near future a cloud of a vast number of wireless devices will be operating at the same time, potentially interfering one another. Ensuring good performance of the deployed wireless networks in this kind of environment is mandatory and obtaining accurate radio propagation estimations by means of a computationally efficient algorithm is a key issue. For that purpose, an in-house three-dimensional ray launching algorithm is employed, which provides radio frequency power distribution values, power delay profiles, and delay spread values for the complete volume of complex indoor scenarios. Using this information together with signal-to-noise estimations and link budget calculations, the most suitable wireless body area network technology for this context is chosen. Additionally, an in-house developed human body model has been developed in order to model the impact of the presence of monitored patients. A campaign of measurements has been carried out in order to validate the obtained simulation results. Both the measurements and simulation results illustrate the strong influence of the presented scenario on the overall performance of the wireless body area networks: losses due to material absorption and the strong influence of multipath components due to the great number of obstacles and the presence of persons make the use of the presented method very useful. Finally, an android-based application for the monitoring of patients is presented and tested within the emergency room scenario, providing a flexible solution to increase interactivity in health service provision.

Keywords

e-Health, patient monitoring, emergency room, ZigBee, wireless body area networks, three-dimensional ray launching

Date received: 10 March 2016; accepted: 7 August 2016

Academic Editor: Alessandro Nordio

Introduction

In recent years, Internet of Things (IoT)[1] has emerged supported by new wireless technologies and the possibility of implementing small, low cost, and reduced energy-consuming devices. IoT proposes a world where everything can communicate with everything, creating

[1]Department of Electrical and Electronic Engineering, Public University of Navarre (UPNA), Pamplona, Spain
[2]School of Engineering and Sciences, Tecnologico de Monterrey, Monterrey, Mexico
[3]Department of Mathematical Engineering and Computer Science, Public University of Navarre (UPNA), Pamplona, Spain

Corresponding author:
Peio Lopez-Iturri, Department of Electrical and Electronic Engineering, UPNA, Campus de Arrosadia, Pamplona 31006, Navarre, Spain.
Email: peio.lopez@unavarra.es

intelligent environments capable of providing great number of potential applications as safety in buildings,[2] sustainability in smart cities,[3] and Geo-related applications,[4] among many others. One of the environments that can take more advantage of the IoT is the medical one, where, thanks to wearable wireless devices, an efficient patient monitoring can be carried out. This leads to the concept of e-Health, which is defined as the recollection and interchange of medical information through electronic devices and digital communication networks to provide essential information to doctors or users for the achievement of a best diagnosis and a fast action in case of emergency. To make this possible, a significant amount of technologies must work together to offer a transparent, or at least the less obstructive possible service for the end user. This ease in usability must be reached in different levels, starting from the development of small-scale devices, enabling straightforward integration with user apparel. In this sense, wireless technologies which enable freedom of movements to users are essential. Taking this into consideration, energy usage profiles must be as efficient as possible to use small batteries and to reduce recharge times.

Based on these premises, some research prototypes have already been developed and implemented on textile or on conventional materials. These prototypes are capable of measuring and monitoring a wide variety of physiological parameters. As an example, in Lopez et al.,[5] a device uses textile sensors to obtain information about location, electrocardiogram (ECG), heart rate, and body temperature in hospital environments. In Melo Tavares et al.,[6] a textile device is also used for monitoring sleep movements and detecting neurodegenerative diseases such as Alzheimer and Parkinson. Regarding the transmission of the medical data acquired by those sensors, the most important wireless systems are wireless body area networks (WBANs),[7–11] where different wireless technologies are employed to transfer the sensed data to portable devices such as a tablet and a mobile phone, where the data will be stored and could be analyzed by a specific software capable of processing and showing all this information in the best way depending on the kind of information and end user. ZigBee,[12] Bluetooth,[13] or radio frequency identification (RFID)[14] are the most widely used communication technologies in this application area, the flexibility and energy autonomy offered by some of them being essential. But for remote monitoring applications, standalone WBANs usually require gateways to other wireless networks in order to have access to databases that will process the acquired data. In this sense, the proliferation of smartphones has solved this issue partially, since most users have a device with multiple connectivity possibilities (Bluetooth, WiFi, High Speed Packet Access (HSPA), etc.). In fact, nowadays, the most widely extended schema is the one that uses mobile phones as gateways.[15,16]

All these wireless technologies and e-Health devices proposed for patient remote monitoring usually operate in complex indoor scenarios in terms of radio propagation, such as hospital rooms and areas, and a patient's home.[17,18] In these scenarios, the placement of the different devices that integrate the wireless communication system can determine the correct performance of the entire system. The fact that the human body is necessarily involved in the scenarios increases the complexity of the communication system analysis. Therefore, the theoretical study of WBANs using simulation tools aids to determine their feasibility as well as to improve the performance of the wireless system. In fact, the deployment of WBANs in indoor scenarios has been studied from different points of view in several works. In Roblin,[19] several WBAN indoor scenarios are studied through the measurement of power delay profile (PDP). In AbuAli and Hayajneh,[20] empirical path-loss model and the measurement results are compared for different human parts and postures considering a ZigBee sensor network. Finally, in Roblin and Wei,[21] statistical WBAN channel characterization is carried out using a complete homogeneous body phantom.

In this work, an e-Health application for medical environment is presented, where useful information for patients, hospital manager, and health personnel is managed. Since hospital environments are complex and the performance of the systems depends strongly on the performance of the wireless sensor network (WSN) interacting with human bodies, a three-dimensional (3D) ray launching (3D RL) simulation tool has been employed with the aim of studying the behavior of potential wireless e-Health devices of a WBAN, deployed on an in-house developed human body model within the scenario. This simulation tool provides an adequate balance between computational cost and accuracy,[22] comparing to full-wave methods which need a great deal processing time and to empirical methods which are less accurate and unsuitable for this type of complex indoor scenarios.[23]

The article is organized as follows: section "Simulation tool and obtained results" introduces the 3D RL tool and the simulated scenarios as well as the employed human body model. An extensive study of obtained results, where different WBAN systems are analyzed, is also carried out; section "Measurement results" shows the measurement results and their comparison with estimations obtained by means of the 3D RL method; section "Hospital e-Health application" introduces medical application; sections "Discussion" and "Conclusion" provide discussion of the results and the conclusions, respectively.

Simulation tool and obtained results

As aforementioned, a deterministic 3D RL simulation technique, in combination with a simplified human body model, has been used to analyze the radio propagation characteristics within hospital scenarios. This simulation tool has been completely implemented and developed in the Public University of Navarre and it has been widely tested[24–26] showing good estimation performance. The presented method is based on geometrical optics (GO) and uniform geometrical theory of diffraction (UTD). The GO approach is able to accurately calculate field contributions taking into account the reflection and refraction phenomena according to the well-known Snell's law, but further propagation of diffracted rays is not considered in this method. Because of that, it is necessary to consider diffraction phenomena to obtain accurate results. Thus, the implementation of diffracted rays according to the UTD concept has been done in the RL approach, leading to more accurate results. It can be found in Azpilicueta et al.[27] that the proposed hybrid GO–UTD algorithm yields excellent results, and that the UTD extension definitely improves the simulations of the RL approach for realistic environments.

When a scenario is simulated, the wavefront produced by a transmitting antenna is discretized, dividing it in a previously set number of rays, which depends on the angular resolution (expressed in spherical coordinates (θ, ϕ)) that is specified by the user. Once the rays have been launched, they spread across the scenario, losing energy as they propagate and collide with the objects within the scenario. Then, diffraction, refraction, and reflection rays are calculated. The adequate consideration of the dielectric properties of the different objects inside the indoor scenario is crucial in order to obtain accurate simulation results. Therefore, dielectric constant and conductivity of all the constitutive materials of the scenario have been carefully chosen and introduced in the algorithm, which have been obtained at the frequency of operation of the wireless system from Komarov.[28] In order to obtain estimations of the energy received in the complete scenario, it is divided in a discrete number of parts (cuboids), linked to inherent limitations given by spatial resolution. When a ray reaches a cuboid, its information is saved, allowing further studies such as the received power level, PDPs or delay spread values, among others.

With the aim of considering the influence persons in overall system operation, a simplified human body model has been developed and coupled to the 3D RL code, taking into account all the dielectric properties that characterize the different constitutive tissues. This simplified model has been widely tested,[29,30] where good accuracy has been obtained comparing both the simulation and measurement results. Considering previous results, in this work only the dielectric properties of the skin tissue have been considered, avoiding the division of the human body in smaller tissue parts that would lead to greater processing load. Dry skin dielectric properties take the values of dielectric constant $\varepsilon_r = 38$ and conductivity $\sigma = 0.95$ S/m for the considered operating frequency (2.4 GHz).

Table 1. Ray launching simulation parameters.

Frequency	2.41 GHz/868 MHz
Transmitter power	10 dBm/18 dBm
Max. reflections permitted	6
Vertical plane angle resolution $\Delta\theta$	1°
Horizontal plane angle resolution $\Delta\varphi$	1°

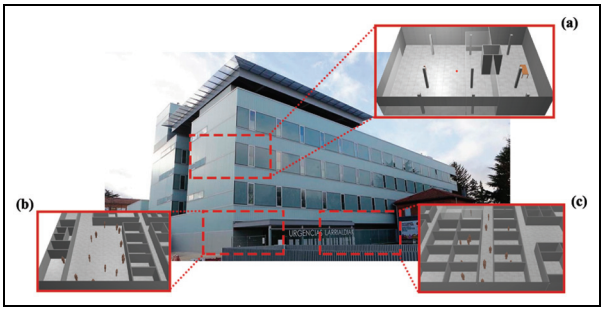

Figure 1. Outdoor of the emergency area of Hospital of Navarre and simulated areas on the (a) first floor and ground level, (b) entrance hall, and (c) medical boxes.

The developed human body model has been configured with a height of 1.8 m, with the rest of the body following conventional proportions, as it is explained in Aguirre et al.[29]

Different industrial, scientific, and medical (ISM) frequencies and transmission power levels have been used in the simulations based on the characteristics of WBAN technologies. In Table 1, all the parameters used in simulations are shown. It must be pointed out that these parameters have been chosen according to a convergence analysis of the algorithm which can be found in Azpilicueta et al.[31]

The simulated scenarios are located in different areas of the emergency building of the Hospital of Navarre, in the city of Pamplona. In Figure 1, the outdoor of the building as well as three areas that have been simulated is shown. The smaller area (Figure 1(a)) is used to analyze the operation of a WBAN communication system attached to the human body and the difference among the different possible placements of the device. On the other hand, the largest one (Figure 1(b) and (c)) is used for the study of the deployment of different WBAN technologies in a complete floor of the building. These scenarios are formed by concrete

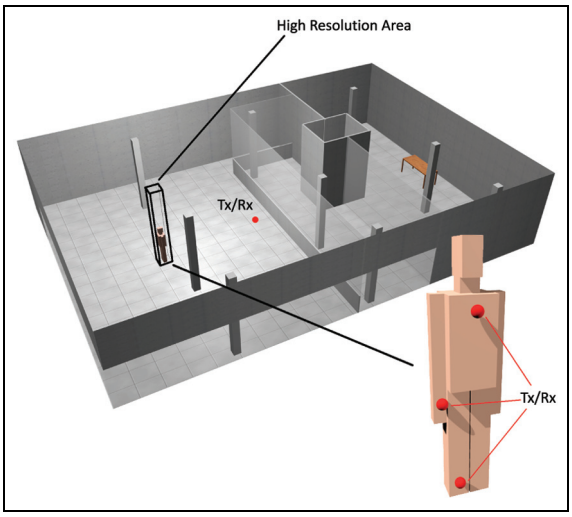

Figure 2. 3D ray launching schematic view of the simulated scenario, where the placements of the used antennas are represented (red points). The high-resolution area around the human body model is also highlighted.

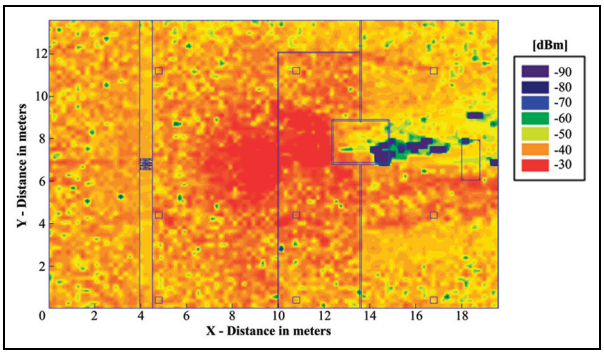

Figure 3. Bi-dimensional power distribution in a constant height horizontal cut-plane, with the scenario schema superposed when the antenna in front of the human body is emitting.

pillars, plasterboard walls, glass walls, and glass windows, and therefore, the dielectric properties of all these materials have been introduced in the simulator for the frequency of operation.

Figure 2 depicts the first part of the scenario which has been considered. Dimensions of this scenario are 19.6 m × 16.6 m × 3.8 m and it has been divided into two different areas. On one hand, a high-resolution are around the human body model is defined (0.55 m × 0.55m × 3.8m), and on the other hand, a lower-resolution are is defined for the rest of the scenario. The high-resolution area is divided into cuboids of 0.03 m × 0.03 m × 0.03 m and the low-resolution area is divided into cuboids of 0.2 m × 0.2 m × 0.2 m. This configuration enables the realization of a more accurate study of the proximities of the human body model. Besides, the lower-resolution for the rest of the scenario decreases significantly the required computational time and avoids inherent RL problems such as divergence.

Different situations have been studied in order to consider an entire communication device. On one hand, a transmitter has been placed in front of the human body at a height of 0.7 m (the red point located in the room depicted in Figure 2), emulating the electromagnetic power generated by a possible ZigBee gateway. On the other hand, different transmitters have been placed in different parts of the body, simulating possible vital sign capturers, for example, a pulsometer or a pacemaker. The transmitter emites 10 dBm RF power and operates at 2.41 GHz frequency band, which corresponds to the ZigBee channel C.

In Figure 3, the simulation results when the antenna is located in the front section of the human body are depicted. Since power distribution is not uniform, the consideration of the different phenomena involved in radioelectric propagation is noticeable, with special relevance of multipath propagation components. The influence of the largest object inside the scenario is also visible considering that the metallic box belongs to the placement of the elevator.

Evidently, the area where more power is received is next to the antenna, although most part of the scenario, including where human body is located, receives enough power to allow a wireless communication. In Figure 4, the received power in three transmitter-to-receiver radial lines is depicted taking into account that the receivers are placed in the ankle, wrist, and chest. These lines start in the antenna area and represent the values obtained between this point and the points where the receivers are placed.

In Figure 4, the received power level in a linear path between the human body and the antenna is depicted. Note that human body placement corresponds to X-axis value of 4 m and the antenna placement corresponds to X-axis value of 8.5 m (corresponding to the deployment shown in Figure 2). The multipath behavior of the propagated electromagnetic wave is more noticeable since the decrease in power does not exhibit a monotonically decreasing trend; in other words, it depends not only on the distance but also on the multipath propagation, corresponding therefore to fast fading phenomena. It is also worth noting that the power values are higher than the receiver sensitivity thresholds of ZigBee devices (−100 dBm), and therefore, as it was predictable considering Figure 3, downlink communication is feasible.

In order to account for the impact of scenario complexity (provided by the number and density of

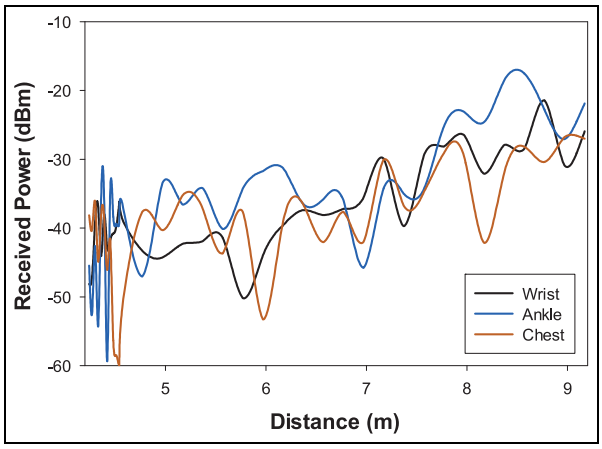

Figure 4. Received power versus linear distance for three different heights when the antenna placed in front of the body is emitting (see Figure 2).

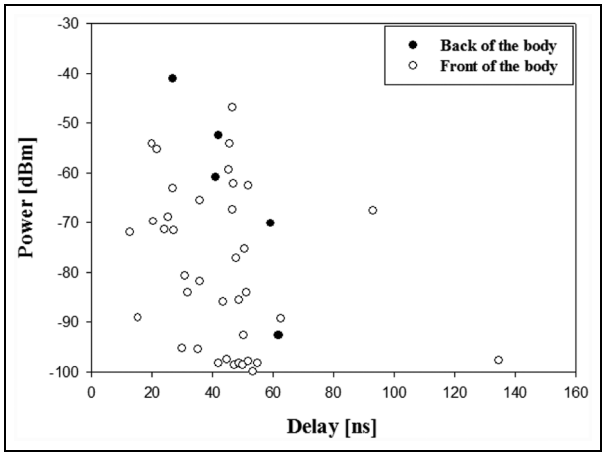

Figure 5. Power delay profile estimations considering two points located in front and behind the human body model.

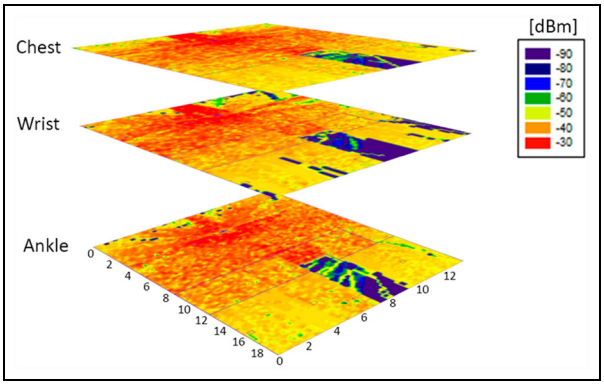

Figure 6. Bi-dimensional power distribution through the scenario when antennas situated in chest, ankle, or wrist are emitting.

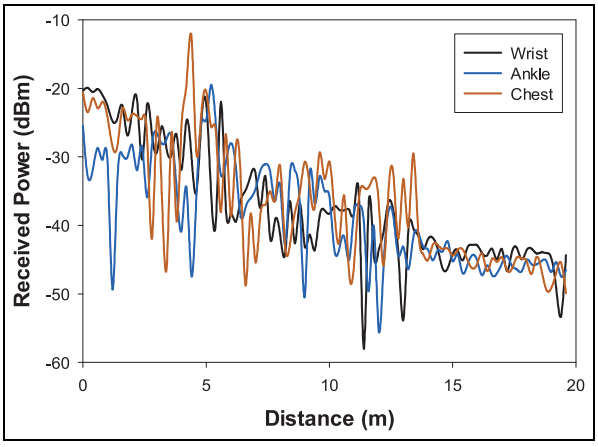

Figure 7. Received power versus linear distance when the three antennas attached to the human body are emitting.

potential scatterers) as well the role of transceiver location, estimations of PDP have been computed. PDPs are an adequate tool in order to estimate scenario complexity and the role of multipath propagation, due to the fact that it provides the distribution of signal power received over a multipath channel as a function of propagation delays. Figure 5 shows PDP estimations for two different positions: at a height of 1.2 m at the back of the human body, and at a height of 0.8 m in front of the human body.

The influence of the human body is visible in PDP since the received rays are more numerous when the antenna is located in front of the body. This circumstance is caused by the dispersive nature and the high absorption rate of the human body, which absorbs most of the energy of the rays that collide with it, creating the known shadow effect.

The next step is to consider the upload link, that is, simulate the power distribution when emitters are placed on different parts of the human body. In Figure 6, the RF power distribution for a bidimentional plane at height 1.27 m is depicted. The cases of an emitting antenna placed on the chest, ankle and wrist are represented.

The influence of the human body is noticeable when the three bi-dimensional received power level planes are compared; the antenna emitting from the right chest produces less energy in the left part of the scenario as a consequence of the human body absorption and dispersion. On the other hand, since the chest antenna is situated on the middle of the body, low power areas generated behind it are more symmetric than the other two cases.

However, that difference is more visible when a transmitter-to-receiver received power level linear distribution with distance is depicted as in Figure 7, where points are obtained at 1.2 m height from the beginning to the end of the scenario and the power received for the three antennas is represented. The difference is

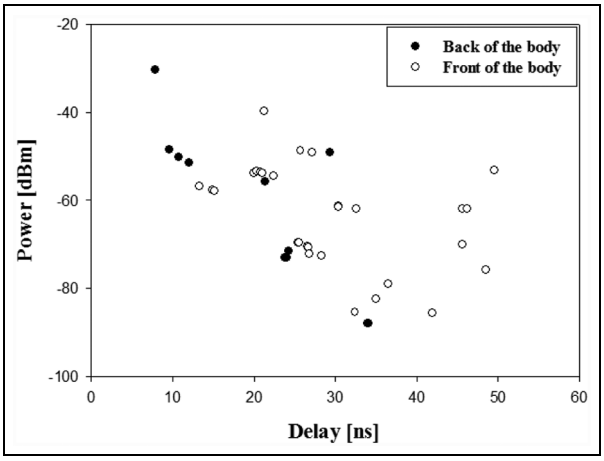

Figure 8. Power delay profile estimation for a point located in front of the person and behind the person when the antenna located in chest is transmitting.

evident, and in fact, when the antenna is placed in chest, the received power level is higher than in the other two cases, taking into account that the selected height is similar to the antenna location height. The influence of the elevator case is also visible in the last part of the graph where the received power decreases considerably.

In Figure 8, PDP estimation values are depicted for the same observation points used previously, but in this case emitting with the antenna placed on the chest. Comparing both PDP values, it can be seen that in this case more rays reach the backside of the human body, given by the proximity of the transmitter to this zone. However, the global contribution is less numerous since the human body absorbs a large amount of the generated power due to its proximity.

Finally, the delay spread estimation, corresponding to the absolute value of the time difference between the arrival of the first and last rays in each point of the scenario, is depicted in Figure 9. The influence of the human body can be seen, as a higher number of rays arrive to the front and sides of the human body; in fact, the concentration of rays in the walls at right and left of the human body can be clearly observed.

For the last two areas, the ground level of the hospital has been simulated (Figure 1(b) and (c)), introducing people in different zones. Two body models, one in an aisle and a second one in a medical box, have been equipped with transmitters attached to their wrists, configuring them with a transmission power of 10 dBm. Besides, two more antennas have been introduced in the entrance hall and in medical box area as gateways with 18 dBm transmission power. The dimensions of this scenario are of 63 m $\times$ 52 m $\times$ 3 m and are divided into cuboids of 0.5 m $\times$ 0.5 m $\times$ 0.5 m. Ninety rooms of different sizes are distributed in the scenario, separated by concrete walls. Human body models have been introduced in the two aforementioned areas as it can be seen in Figure 10.

Power distributions for the previously described antennas are depicted in Figure 11. In this case, the influence of the scenario is relevant; the power generated by the first antenna, which is placed in a larger room, expands into a larger area. Although the second and third antennas are in the same aisle, they exhibit different behaviors due to the different heights at which they are placed and the higher transmission power level of the second antenna.

Once the received power distribution from the proposed transceiver locations has been obtained, the performance of the wireless links can be assessed in terms of signal-to-noise ratio (SNR). As an example, the two wearable transceivers placed on the wrists of the patients and the node placed on the ceiling of the medical boxes zone have been evaluated (see Figure 10(c)). Both the uplink (from wearable mote to

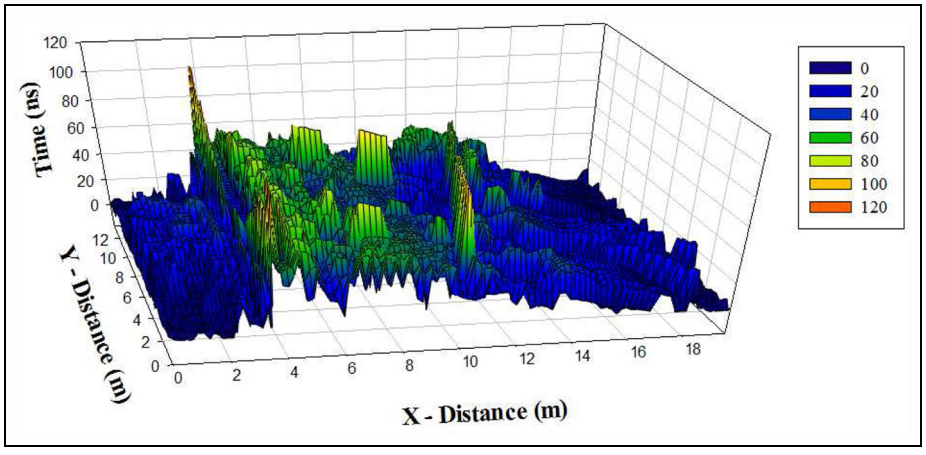

Figure 9. Delay spread for the height of 1.2 m when the antenna situated in chest is emitting.

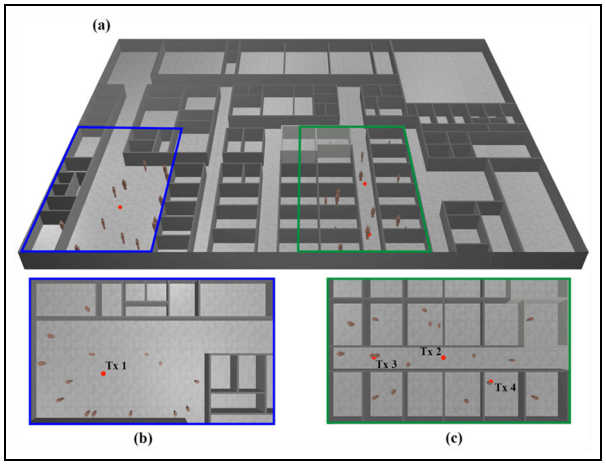

Figure 10. (a) Background floor of the emergency area of the Hospital of Navarre, (b) entrance hall, and (c) and medical boxes.

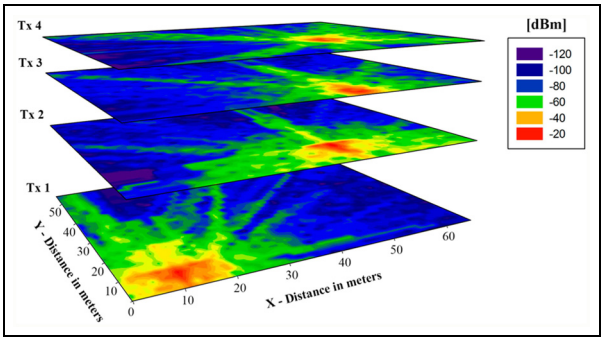

Figure 11. Received power distribution for four transmitting antennas, two attached to human bodies and two placed in the ceiling of entrance hall and a medical box.

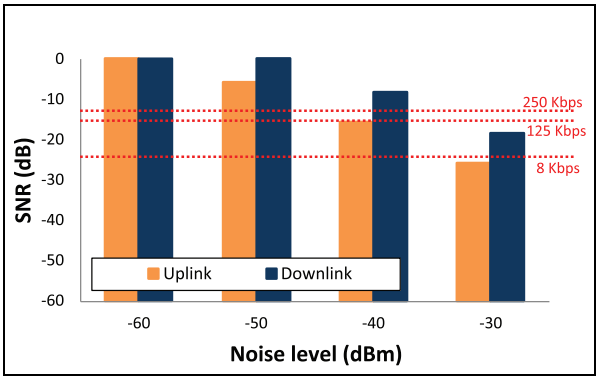

Figure 12. SNR values for the case of the patient within the aisle for different noise levels.

fixed node) and the downlink (from fixed node to wearable mote) communications have been analyzed. In Figure 12, the SNR values for the wireless communication link between the node placed on the ceiling and the patient within the aisle are shown. Figure 13 represents the same, but for the case of the patient within the medical box. The red dashed lines show the minimum SNR required for a successful communication at the indicated bit rates. Although the data rate for ZigBee communications is 250 kbps, other data rates have been taken into account in the study in order to gain insight into the effect of the noise on different configurations. These required minimum SNR values (represented by red dashed lines in Figures 12 and 13) have been calculated by the following well-known Shannon's equation

$$C = BW \times \mathrm{Log}_2\left(1 + \frac{S}{N}\right) \quad (1)$$

where C is the capacity of the channel (bps), BW is the channel bandwidth (3 MHz for ZigBee), and S and N are the received signal and noise power levels, respectively. First, is it worth noting how the SNR values of the uplink are lower than the values of the downlink for both Figures 12 and 13. This is mainly due to the transmitted power differences between the wearable device and the fixed node at the ceiling. This fixed node has been configured to transmit 18 dBm, but the wearable has been configured to transmit 10 dBm in order to reduce the power consumption as it has to be powered by a battery. Besides, the maximum transmitted power level for this kind of communications in some countries (e.g. in Europe) is 10 dBm. Another interesting result is that the SNR values are lower for the communication with the patient within the medical box. Although the noise levels have been supposed the same for Figures 12 and 13, the received power level when the patient is within the medical box is lower due to the higher presence of obstacles between the transmitter and the receiver. Finally, as it can also be observed in the figures, the most relevant effect is the influence of noise (i.e. electromagnetic interferences) present in the scenario, which will have a great impact on the performance of the deployed WSN. Depending on the data rate required by the application running over the WSN, a minimum SNR value will be required, which could not be achieved. For example, the case of –40 dBm of background noise shown in Figure 12: if the wireless network needs to transmit at 250 kbps, the downlink will do it successfully (the SNR value is higher than the threshold), but the uplink will fail, as the SNR value is scarcely above the 125 kbps threshold. A solution for this situation is increasing the transmitted power, but it will lead to higher consumptions of the wireless motes. Figure 14 shows the effect of varying the transmitted power level for the mentioned case of -40 dBm of noise level from Figure 12. The graph shows how the obtained SNR values can be improved by increasing the transmitted power of the wireless motes, being decisive in many cases in order to achieve specific bit rates.

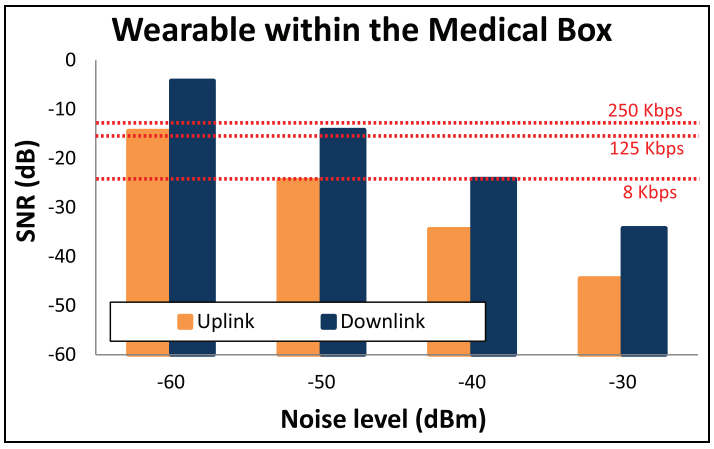

Figure 13. SNR values for the case of the patient within the medical box for different background noise levels.

One of the most widely extended WBAN technologies is RFID thanks to its system architecture, where data are only sent when the reader interrogates the tag for the information, thus saving energy. Two kinds of tags are defined, active and passive tags. Passive tags use the received electromagnetic energy to feed its circuits and then send the desired signal, and active tags are fed by batteries. When passive tags are used, link budget must be calculated to determine whether the link is feasible and the received power in the reader is higher than its sensitivity. Link budget is defined by the following formula[32]

$$\begin{aligned} P_{r,reader}(\text{dBm}) &= P_{reader}(\text{dBm}) + 2G_{reader}(\text{dB}) \\ &- 2L_{sys}(\text{dB}) + 20\log|\rho'| + 2G_{tag}(\text{dB}) \\ &+ 2\Delta G(\text{dB}) - L_{pu} - L_{pd} \end{aligned} \tag{2}$$

where $P_{reader}(\text{dBm})$ is the transmission power of the reader, G_{reader} is the gain of the reader, L_{sys} is the contribution due to system losses (wires, electronics, etc.), ρ' is the decoupling coefficient, G_{tag} is the gain of the tag, $\Delta G = G_{tag}(\text{dB}) - G_{tag,freespace}$ and L_{pu}, L_{pd} are the power lost caused by the propagation in the uplink and downlink, respectively. Therefore, link budget considers losses and gains findable in the different steps of the wireless communication process to determine the feasibility of the communication with a passive RFID device, taking into consideration these variables not only in downlink but also in uplink.

In this case, new simulations have been carried out considering RFID system characteristics: an operating frequency of 868 MHz and a power transmission level range from 10 to 21 dBm (which corresponds to typical commercial RFID readers). The scenario (Figure 10) has been studied and both transmitter T × 3 and T × 4 have been considered as passive tags with a typical sensitivity of 2 dBi. In Figure 15, the obtained link budget values for the mentioned transmission power rate are

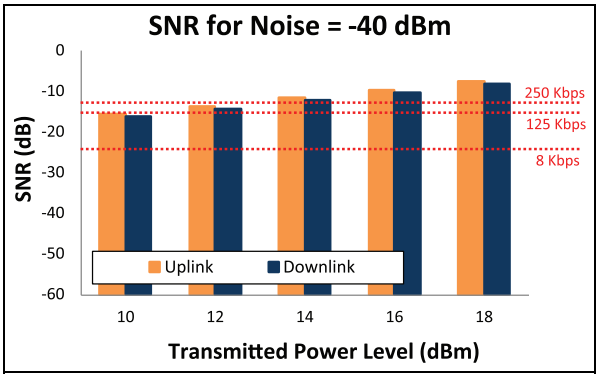

Figure 14. SNR values for different transmitted power levels for the case of the patient within the aisle and a noise level of −40 dBm.

depicted as well as the reference levels for minimum sensitivity given by four commercial RFID readers.

As it is shown in Figure 15, from the point of view of received power level, transmission is only successful when the transmitter is placed in the medical box area, since only reader 2 overcomes sensitivity level. This is caused by the distance (reader 1 is in the entrance hall) and the topology of the scenario together with the fact that RFID is a narrow area communication system if it is compared with other WBAN systems such as ZigBee and Bluetooth.

Finally and based on ISM 2.4 GHz simulation results, the analysis of the deployment of two different communication systems, ZigBee and Bluetooth, has been performed in the considered scenario. Specifically, the wireless devices that have been evaluated are ZigBee XBee Pro and ZigBee XBee transceivers from Digi International Inc. The main differences between them are the larger transmitter power of XBee Pro and its longer-range distance. In order to analyze the worst-case conditions, the minimum default value of the

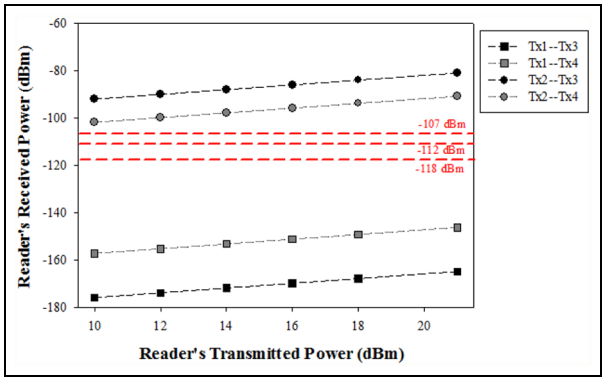

Figure 15. Link budget estimation including sensitivity reference levels and considering Tx3 and Tx4 as RFID tags.

Table 2. Parameters for the different considered wireless communication systems.

	Transmitted power (dBm)	Sensitivity (dBm)
ZigBee XBee Pro	10	−100
ZigBee XBee	10	−92
BLE		
Minimum transmitted power	−20	−93
Maximum transmitted power	10	−87
Bluetooth Class 1	20	−90
Bluetooth Class 2	4	−90
Bluetooth Class 3	0	−90

BLE: Bluetooth low energy.

transmitted power level has been considered. Bluetooth low energy (BLE) and classic Bluetooth have also been evaluated. The transmitted power and sensitivity for the different communication systems considered[33] are shown in Table 2.

Figure 16 shows the linear distributions of received power along the X-axis and Y-axis for different values of Y and X, for the different technologies, with the sensitivity of each of them.

From Figure 16, it can be seen that there are several locations where the signal goes down below the sensitivity level, given by site-specific fading mainly due to multipath propagation. With these values, an optimal design of the WSN coverage can be obtained, as shown in Figure 17 for the different technologies. The results show that coverage/capacity estimations are dependent on the overall interference level, which, in turn, is a function of wireless propagation characteristics, which are site specific as well as device specific. In this sense, it is worth noting that the overall interference levels will be given by intra-system (i.e. users served by the same access point or gateway), inter-system (from other communication systems, within the operating bandwidth of the functional system in operation), or background noise. Therefore, parameterization of transceivers (in terms of transmission power, transmission mode, or employed radiating elements) will play a key role in these overall interference levels. The proposed deterministic analysis can therefore aid in the estimation of the adequate network topology to deploy, as well as in the proposal of transceiver parameters of operation.

Measurement results

Once the theoretical study of the scenario has been carried out, as well as the radio-planning estimations in terms of coverage/capacity relations, the measurements are performed and compared with the simulation results of the first scenario (Figure 1(a)). With this aim, the aforementioned locations of the antenna have been used, considering a transmitter placed in front of the person and three transmitters placed on the chest, wrist, and ankle, as shown in Figure 2. The utilized devices are communicated by means of ZigBee technology, and in fact, these devices are XBee Pro motes by Digi International. The antenna used has been a whip antenna with a gain of 1.5 dBi mounted on the XBee Pro RF module, with a radiation pattern similar to that of a dipole. The XBee Pro RF modules have been attached to the different parts of the body with scotch tape for the purpose of the different measurements.

At the other end, an Agilent N9912A Fieldfox RS field Analyzer is used to measure the received power once the transmitters are emitting. This powerful device allows an accurate estimation of the electromagnetic power that reaches each measured point. The different parameters that take part in the wireless communication, as antenna gain or the frequency of operation, have been the same (see Table 1) as in the 3D RL simulations in order to obtain a fair comparison between the simulation results and measurements.

First, the antenna is placed in front of the test person and the received power in the three different locations is measured (Table 3) simulating the downlink and obtaining a mean absolute error of 4.11 dB and a relative error of 8.6%, showing good agreement between the measurement and simulation and validating the use of the 3D RL simulation tool.

In Table 4, the uplink is emulated, placing the antenna in chest ankle and wrist and measuring the received power in front of the person. Even though the error has been duplicated in comparison with the downlink, it is still within the margins considering that the absolute mean error have a value of 7.35 dB and the relative shows an error of 15.9%.

Hospital e-Health application

The concept of traceability of both control assets and instruments in the hospitals has been developed for

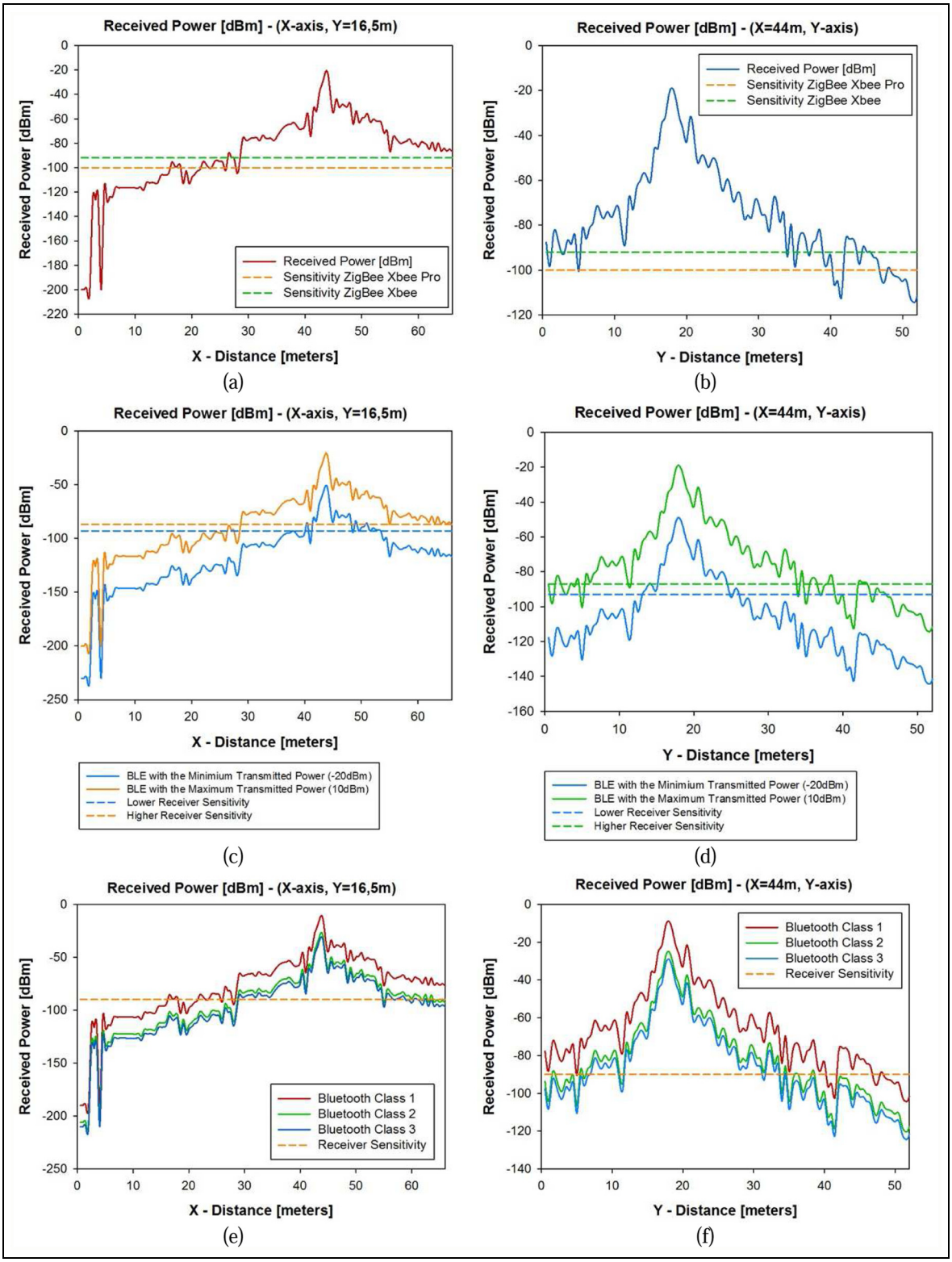

Figure 16. Comparison of radials of received power (dBm) along the *Y*- axis and *X*-axis for the considered scenario with the receiver sensitivity: (a) ZigBee XBee Pro and ZigBee XBee along the *X*-axis for *Y* = 16.5 m, (b) ZigBee XBee Pro and ZigBee XBee along the *Y*-axis for *X* = 44 m, (c) BLE along the *X*-axis for *Y* = 16.5 m, (d) BLE along the *Y*-axis for *X* = 44 m, (e) classic Bluetooth along the *X*-axis for *Y* = 16.5 m, and (f) classic Bluetooth along the *Y*-axis for *X* = 44 m.

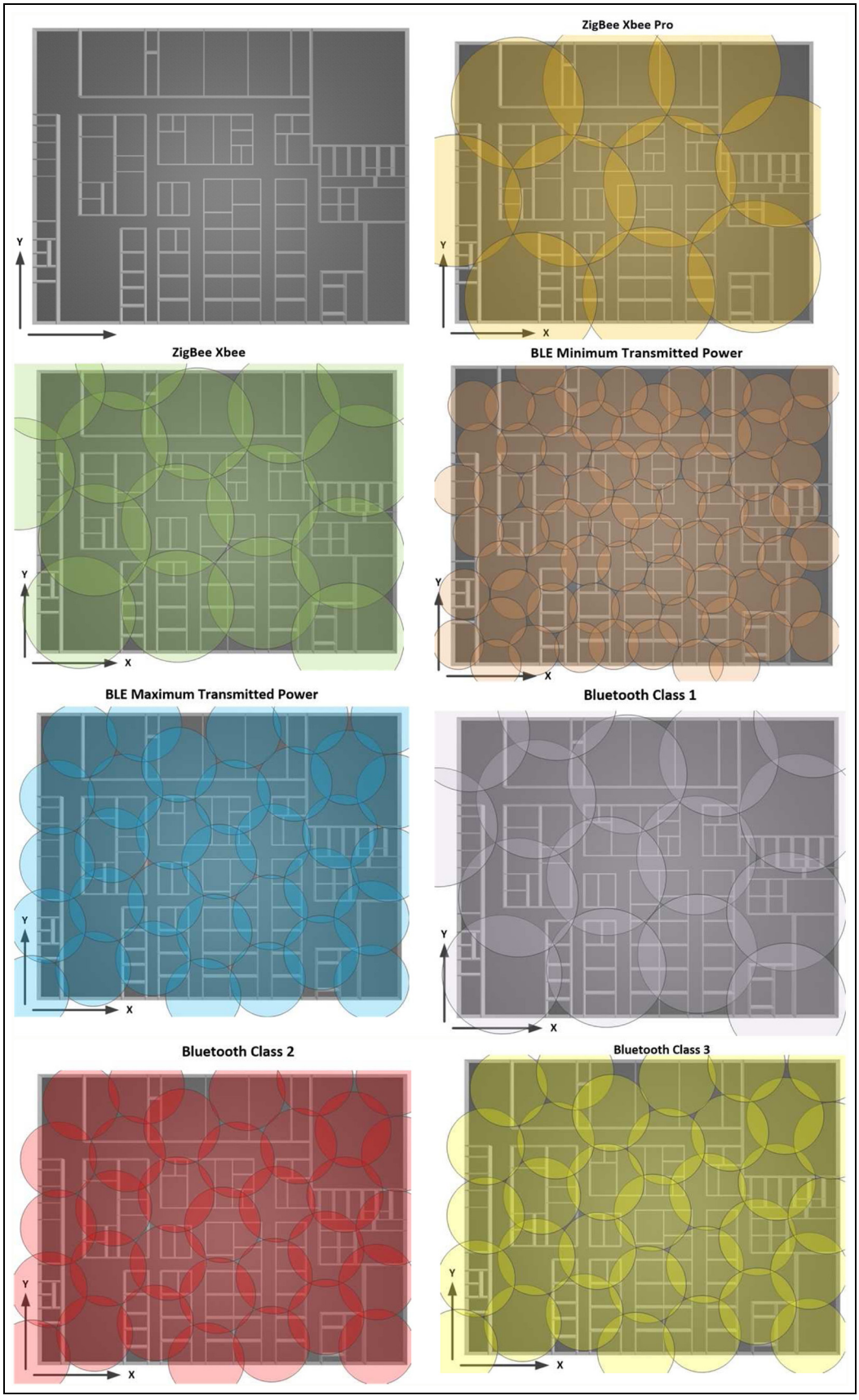

Figure 17. Radio-planning coverage for different technologies within the considered environment.

Table 3. Comparison between the power received and measurement results in three locations of the human body when antenna is placed in front of it.

Antenna RX	Simulation results	Measurement results
Ankle (0.16 m)	−46.18 dBm	−42.35 dBm
Wrist (0.84 m)	−49.21 dBm	−44.39 dBm
Chest (1.27 m)	−48.11 dBm	−44.43 dBm

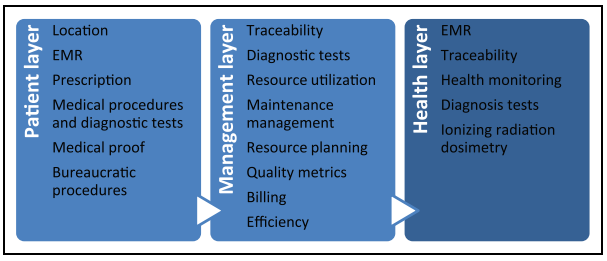

Figure 18. Application layers' description.

years, but now this also applies to users. This type of monitoring makes the management of the information flow much easier and ensures its faster and safer acquisition. Traceability, considered as the ability to verify the history, location, or application of an item by means of documented recorded identification, may also apply to the health personnel (physicians, nurses, etc.), patients, and management staff of a hospital.

The quality of healthcare service provision may increase significantly applying traceability technologies, as well as business intelligence (BI) tools, to identify and monitor the indicators to assess the management of hospitals and set new goals (strategic plans). Traceability of medical personnel and patients not only improves the management of hospitals but also allows the delivery of medical reports to the relatives of the patients (if they so request) and the debugging of legal responsibilities (applicable in some instances) and the increase in satisfaction and trust of patients.

Hospitals, which may be considered in this sense as smart logistics centers, may consider some monitoring technologies already used by logistics companies (as RFID), but the value added is in real and operational integration of intelligent devices in the process of acquiring and managing information. At the management layer, traceability of people at hospitals allows the development of reports on the work performed, the person in charge of handling an alarm, the person in charge of handling a given patient, the time required to accomplish a given task, the number of patients seen by a physician, the number of patient visits per hour, and even more.

Concerning health issues, physicians are more interested on the vital signs of patients. Those parameters are easy to obtain in an intensive care unit, but they are not always reachable from portable devices (as holters, or similar devices). The wait in the emergency department of the hospitals is often long and tedious, consultations with medical specialists are traumatic in some cases, the duration of the diagnostic tests despairs patients, and so on, so the patient layer also requires a special attention. The availability on their mobile devices of certain information in order to facilitate patient waiting, to facilitate the understanding and acceptance of the diagnosis, to calm her or him before the diagnostic tests or medical procedures, or just guide her or him in their travel through the hospital grounds are issues that significantly improve the perception of the patient's medical care dispensed. Figure 18 depicts some of the most relevant issues of each layer.

Following the requirements described above, an application has been developed in order to provide service to patients, health personnel, and management staff. Due to the mobility requirements of our potential users, we have selected a mobile app in order to grant universal access to all of them. The system follows a service-oriented architecture (SoA) with three layers. The lower one is in charge of database connectivity, communication and security providing, data acquisition, storing, integration, and replication. The services of the intermediate layer, which rely on the services of the lower level, provide location and tracking services, data monitoring, dosimetry metrics, resource monitoring, diagnostic information, and estimators for quality metrics. Finally, the upper layer provides high-level services related to BI, electronic medical records (EMRs), resource planification/optimization, quality of service monitoring, billing information, intelligent health monitoring (telemedicine), and electronic prescription. Figure 19 depicts the SoA architecture followed. Services of the upper layer are provided by open source tools such as Pentaho Community v6[34] (BI), dcm4chee (picture archiving and communication system (PACS)), and Open EMR 4.2[35] (EMR), while data storing and replication is provided by a MySQL[36] database server and SymmetricDS.[37]

Figure 20 shows the system architecture, where three database management systems are connected by a network and replicated using SymmetricDS. The whole system has been developed over three Ubuntu 14 Linux servers, three MySQL 5.7 servers, and a data integration/acquisition C++ module that interacts with a set of Waspmote gateways (WiFi, Bluetooth, and IEEE 802.15.4). Data sensors automatically collect the information (holter, event sensor, location, sensor, etc.) and store it into the database. The frequency of data collection depends on the requisites of each application. Vital signs' monitoring requires high-frequency garbage, while location does not. BI and EMR tools work over

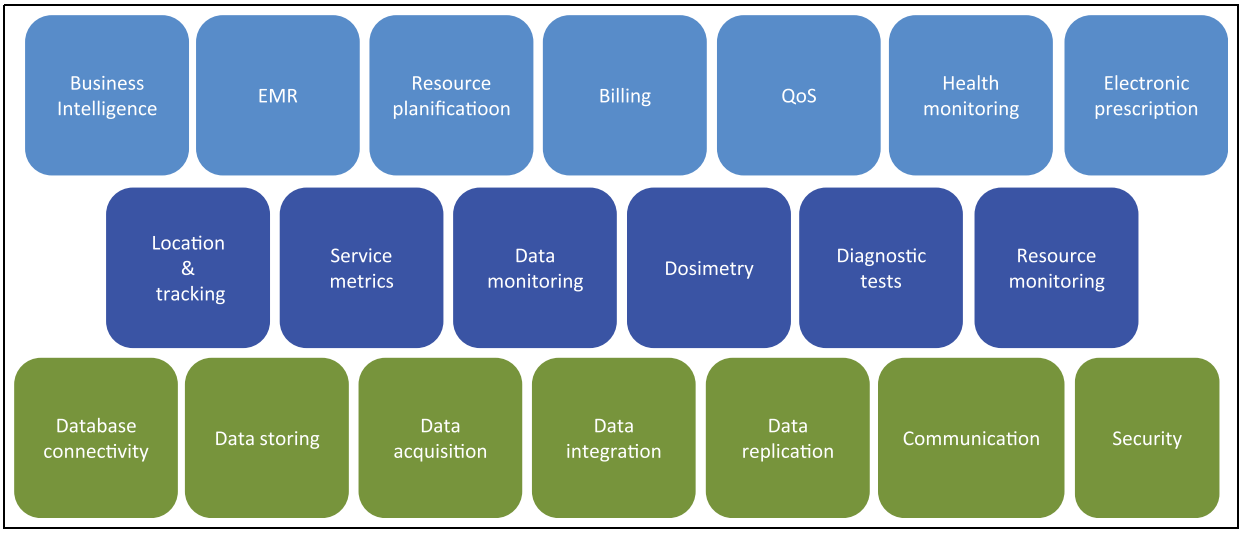

Figure 19. SoA architecture.

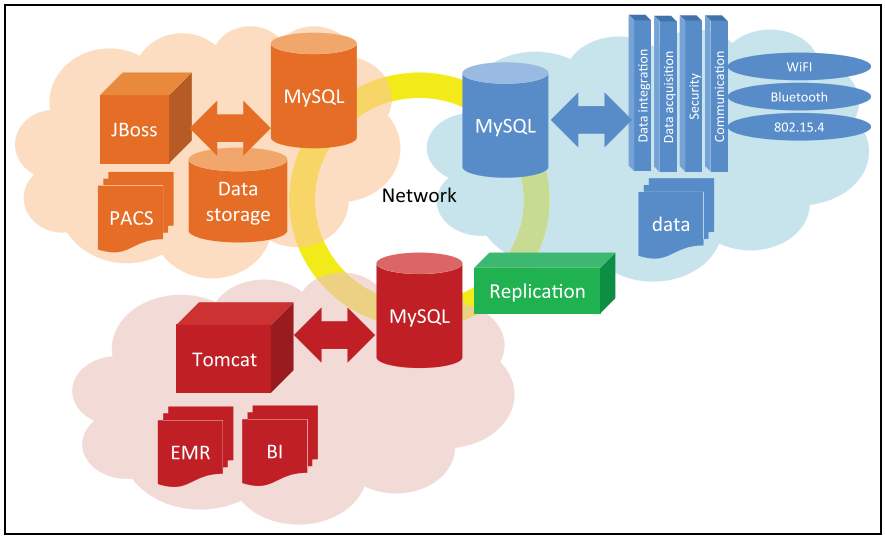

Figure 20. System architecture.

a Tomcat server, while the PACS needs a JBoss server. In order to provide good performances, we apply the principle of locality to the database servers. We assume that each application interacts primarily with its closest database server. However, we use a replication tool (SymmetricDS) to ensure data availability in all the system nodes.

The information stored on the system can be accessed through a mobile application (called Emergency) developed for the Android platform (Android 6, API v23). Figure 21 shows the application interfaces for the patient, health manager, and health personnel. Each user has a profile system access and the interface observed according to this profile gives her or him access to those features whose use is authorized. For example, a patient may access their pharmaceutical prescriptions, her or his clinical diagnostics, administrative documents as doctor's notes, and many more (see Figure 22(a)). The hospital management staff can know in real-time the degree of utilization of the hospital resources, the maintenance activities scheduled and running, the degree of patient satisfaction through quality and satisfaction surveys, and many other features, as shown in Figure 22(b). The BI tool implemented provides a very useful dashboard where hospital staff can monitor hospitalizations, discharge reports, manage appointments, etc. The health personnel can locate a patient by means of a location service based on a fuzzy location inference system and a fuzzy automaton–based tracking system,[38] can also monitor the vital signs of

Figure 21. Application interfaces for the (a) patient, (b) health manager, and (c) health personnel.

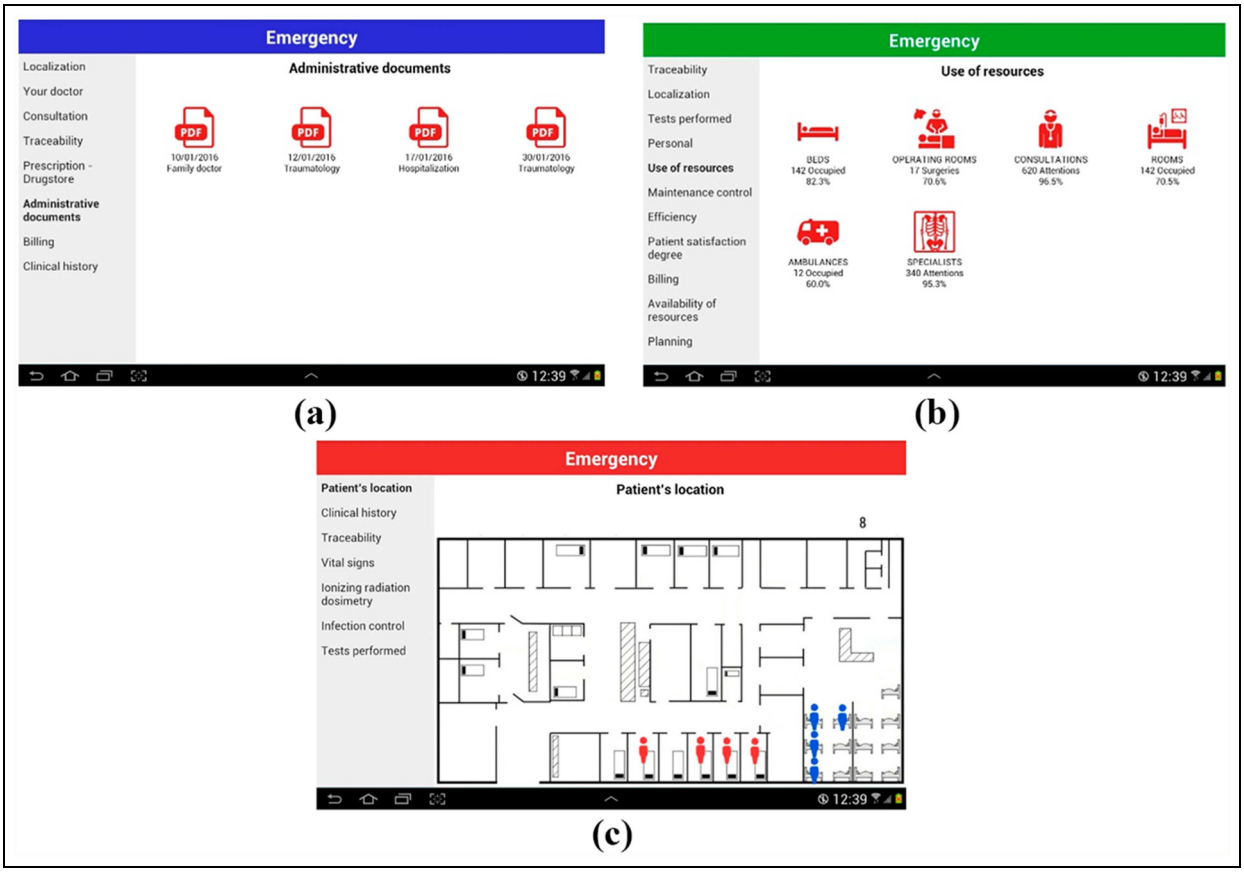

Figure 22. More detailed application interfaces for the (a) patient, (b) health personnel, and (c) health manager.

those patients equipped with event monitors with RF connectivity (Bluetooth, IEEE 802.15.4, and WiFi), can access the EMR of a patient, and so on (see Figure 22(c)).

Some services, such as dosimetry or location and tracking, are event-driven services. That implies a different behavior on the application management. The behavior of the application may be proactive or reactive according to the use of some of those services. For example, the location of a certain patient can be performed on demand when needed, or the system can also monitor his or her location continuously. In this last case, the location service triggers some events to the Android application and it refreshes the user location as he or she moves. The Android app is a front-end application that communicates wirelessly with the services provided by the system. It allows local data storage during possible periods of communication interruption. The occurrence of a total or a partial wireless communication interruption causes a certain

number of retries (configurable). If the problem persists, the application locally stores the data on a serialized file. The application checks periodically if communication has been restored, and if so, it sends the pending information stored locally to the appropriate services and removes the local copy.

Discussion

This study is devoted to prove the feasibility of the implementation of e-Health technologies inside a hospital, developing a patient monitoring application, as well as the advantages of the introduction of deterministic simulation tools in the characterization and implementation of those WBAN-based systems. The chosen simulation tool is known as 3D RL, a method that returns accurate results utilizing low processing times.

The 3D RL simulation tool has demonstrated its potential offering interesting information about the behavior of the radioelectric waves inside a complex scenario as presented in this work. It not only allows knowing the number of transmitter that must be spread along the scenario but also their position for an optimum wireless network.

The flexibility of the simulation tool also allows the easy consideration of different WBAN technologies, changing transmission power or frequency, to adequate the radio-planning to any specific case. For this scenario, simulation tool together with a deep knowledge of the different network topologies has allowed to determine that ZigBee is the best option due to the flexibility, low power consumption, and the high number of devices that can work together. In contrast, RFID is a shorter-range technology and Bluetooth is less scalable. The adequate performance of the code has also been demonstrated when the simulation and measurement results have been compared (Tables 3 and 4) offering a low error rate.

On the other hand, the introduction of a simplified human body model is essential since the considered network is a WBAN, thus allowing the study of its impact and giving the opportunity of implement a realistic system placing devices in different parts of the human body. In fact, a ZigBee communication system is studied taking into account a gateway and three devices situated in chest, wrist, and ankle.

Table 4. Comparison between the power received and measurement results placing the receiver in front of the human body when three antennas situated on person are emitting.

Antenna TX	Simulation results	Measurement results
Ankle (0.16 m)	−48.22 dBm	−54.17 dBm
Wrist (0.84 m)	−45.10 dBm	−53.74 dBm
Chest (1.27 m)	−45.30 dBm	−52.76 dBm

The antennas attached to the person show the high absorption produced by the body (Figure 6), changing completely the power distribution in three cases, especially in areas where there is no direct visibility and therefore, the human body is in the middle of the two points. This behavior is more noticeable when PDP is studied, taking into account the difference between the rays passing through the points situated in front and back of the body (Figures 5 and 8).

Finally, the specific software presented shows an easy way to give real-time information to patients, health manager, and health personnel through common android-based devices. This kind of aid is essential in emergencies since an efficient attending system can improve the overall service and accelerate the diagnosis, avoiding accidents or the existence of untended patients. The huge quantity of data that are managed by the system must be taken into consideration, and therefore, a robust system is developed for this work. In any case, the implementation of an e-Health system based on ZigBee and WBANs within a complex scenario such as a hospital has been demonstrated feasible considering the results of this work.

Conclusion

e-Health is the future of healthcare allowing the simplification of some procedures and increasing the quality of life for many people around the world with their continuous physiological parameter monitoring and offering quick response of medical staff in the cases that it is necessary. The successful implementation of this concept is widely related to WBAN technologies such as ZigBee, Bluetooth, and RFID, which are prepared to offer a flexible communication between devices attached to the human body and their environment. This communication must be studied and characterized as much as possible with the aim of generating optimal e-Health systems.

In this work, a WBAN-based communication system implemented in a complex scenario is studied using a 3D RL method combined with a simplified human body model. The uplink and downlink are studied considering transmitters attached to the human body and in front of it. Power distribution, PDP, and delay spread graphics have been obtained with the aim of studying the behavior of the electromagnetic waves generated by the system and the feasibility of the implementation of the system in this kind of scenarios. Different WBAN technologies have been studied to determine which one is the more adequate for a big and complex scenario such as the presented emergency area of the Hospital of Navarre. To this end, link

budget SNR values and radio-planning graphs have been presented. Real measurements have been obtained and compared with the simulation results, showing good accuracy between them. An android-based application to give information on patients, hospital manager, and personal has also been presented, showing a description of its layer and architecture. Finally and considering the obtained results, it can be concluded that the development of e-Health systems based on wireless WBANs within complex indoor scenarios is feasible. Even more, the aid of a deterministic simulation tool such as the presented 3D Ray Launching method is essential for the improvement and optimization of the performance of the entire wireless system.

Declaration of conflicting interests

The author(s) declared no potential conflicts of interest with respect to the research, authorship, and/or publication of this article.

Funding

The author(s) disclosed receipt of the following financial support for the research, authorship, and/or publication of this article: The authors acknowledge the support received from the Ministry of Economy and Competitiveness, Government of Spain, under grant TEC2013-45585-C2-1-R.

References

1. Coetzee L and Eksteen J. The Internet of Things—promise for the future? An introduction. In: *Proceedings of the IST-Africa conference*, Gaborone, Botswana, 11–13 May 2011, pp.1–9. New York: IEEE.
2. Chen T-Y, Wei H-W, Hsu N-I, et al. A IoT application of safe building in IPv6 network environment. In: *Proceedings of the IEEE 37th annual computer software and applications conference*, Kyoto, Japan, 22–26 July 2013, pp.748–753. New York: IEEE.
3. Kyriazis D, Varvarigou T, Rossi A, et al. Sustainable smart city IoT applications: heat and electricity management & Eco-conscious cruise control for public transportation. In: *Proceedings of the IEEE 14th international symposium and workshops on a world of wireless, mobile and multimedia networks (WoWMoM)*, Madrid, 4–7 June 2013, pp.1–5. New York: IEEE.
4. Dayu S, Huaiyu X, Ruidan S, et al. A GEO-related IOT applications platform based on Google Map. In: *Proceedings of the IEEE 7th international conference on e-business engineering (ICEBE)*, Shanghai, China, 10–12 November 2010, pp.380–384. New York: IEEE.
5. Lopez G, Custodio V and Ignacio Moreno J. Location-aware system for wearable physiological monitoring within hospital facilities. In: *Proceedings of the IEEE 21st international symposium on personal indoor and mobile radio communications*, Instanbul, Turkey, 26–30 September 2010, pp.2609–2614. New York: IEEE.
6. Melo Tavares M, Ramos Belino NJ, Vaz Patto MA, et al. Development of an electroactive textil system for the objective assessment of sleep movements and neurodegenerative diseases. In: *Proceedings of the 1st Portuguese meeting in bioengineering (ENBENG)*, Lisbon, 1–4 March 2011, pp.1–4. New York: IEEE.
7. Lupu C and Cosmin-Constantin M. Actual portable devices as base for telemedicine and e-health: research and case study application. In: *Proceedings of the E-health and bioengineering conference (EHB)*, Iasi, 21–23 November 2013, pp.1–4. New York: IEEE.
8. Hamalainen M, Taparugssanagorn A and Iinatti J. On the WBAN radio channel modelling for medical applications. In: *Proceedings of the 5th European conference on antennas and propagation (EUCAP)*, Rome, 11–15 April 2011, pp.2967–2971. New York: IEEE.
9. Chin CA, Crosby GV, Ghosh T, et al. Advances and challenges of wireless body area networks for healthcare applications. In: *Proceedings of the international conference on computing networking and communications*, Maui, HI, 30 January–2 February 2012, pp.99–103. New York: IEEE.
10. Lee S and Yoo H-J. Low power and self-reconfigurable WBAN controller for continuous bio-signal monitoring system. *IEEE Trans Biomed Circuits Syst* 2013; 7(2): 178–185.
11. Aoyagi T, Takada J, Takizawa K, et al. Propagation characteristics for 2.45 GHz dynamic wearable WBAN using multiport VNA. In: *Proceedings of the 6th international symposium on medical information and communication technology (ISMICT)*, La Jolla, CA, 25–29 March 2012, pp.1–4. New York: IEEE.
12. Rocu MP. Implementation for a WBAN-ECG monitoring system (preliminary results). In: *Proceedings of the international conference on optimization of electrical and electronic equipment (OPTIM)*, Bran, 22–24 May 2014, pp.823–826. New York: IEEE.
13. Wong ACW, Dawkins M, Devita G, et al. A 1 V 5 mA multimode IEEE 802.15.6/bluetooth low-energy WBAN transceiver for biotelemetry applications. *IEEE J Solid: St Circ* 2013; 48(1): 186–198.
14. Malison P, Promwong S, Sukutamatanti N, et al. Indoor measurement and modeling of RFID transmission loss at 5.8 GHz with human body. In: *Proceedings of the 5th international conference on electrical engineering/electronics, computer, telecommunications and information technology*, Krabi, Thailand, 14–17 May 2008, pp.421–424. New York: IEEE.
15. Martínez-Espronceda M, Martínez I, Led S, et al. INTENSA: heart failure patient's follow-up system using the ISO/IEEE11073 standard. In: *Proceedings of the 9th international conference on information technology and applications in biomedicine*, Larnaca, 4–7 November 2009, pp.1–4. New York: IEEE.
16. Rahman MA, Alhamid MF, El Saddik A, et al. A framework to bridge social network and body sensor network: an e-health perspective. In: *Proceedings of the IEEE international conference on multimedia and expo*, New York, 28 June–3 July 2009, pp.1724–1727. New York: IEEE.

17. Aragues A, Escayola J, Martínez I, et al. Trends and challenges of the emerging technologies toward interoperability and standardization in e-health communications. *IEEE Commun Mag* 2011; 49(11): 182–184.
18. Pau I, Seoane F, Lindecrantz K, et al. Home e-health system integration in the Smart Home through a common media server. In: *Proceedings of the annual international conference of the IEEE engineering in medicine and biology society*, Minneapolis, MN, 3–6 September 2009, pp.6171–6174. New York: IEEE.
19. Roblin C. Analysis of the channel power delay profile of WBAN scenarios in various indoor environments. In: *Proceedings of the IEEE international conference on ultra-wideband*, Bologna, 14–16 September 2011, pp.545–549. New York: IEEE.
20. AbuAli N and Hayajneh M. Performance evaluation of channel models of ZigBee sensor networks. In: *Proceedings of the 8th international wireless communications and mobile computing conference*, Limassol, 27–31 August 2012, pp.860–865. New York: IEEE.
21. Roblin C and Wei Y. Scenario-based WBAN channel characterization in various indoor premises. In: *Proceedings of the 9th European conference on antennas and propagation*, Lisbon, 13–17 May 2015, pp.1–3. New York: IEEE.
22. Seidel SY and Rappaport TS. Site-specific propagation prediction for wireless in-building personal communication system design. *IEEE T Veh Technol* 1994; 43: 879–891.
23. Lopez-Barrantes AJ, Gutierrez O, Adana FSD, et al. Comparison of empirical models and deterministic models for the analysis of interference in indoor environments. In: *Proceedings of the Asia-Pacific symposium on electromagnetic compatibility*, Singapore, 21–24 May 2012, pp.509–512. New York: IEEE.
24. Azpilicueta L, Falcone F, Astrain JJ, et al. Measurement and modeling of a UHF-RFID system in a metallic closed vehicle. *Microw Opt Techn Let* 2012; 54(9): 2126–2130.
25. Nazábal JA, Iturri López P, Azpilicueta L, et al. Performance analysis of IEEE 802.15.4 compliant wireless devices for heterogeneous indoor home automation environments. *Int J Antenn Propag* 2012; 176383.
26. Iturri PL, Nazábal JA, Azpilicueta L, et al. Impact of high power interference sources in planning and deployment of wireless sensor networks and devices in the 2.4 GHz frequency band in heterogeneous environments. *Sensors* 2012; 12(11): 15689–15708.
27. Azpilicueta L, López-Iturri P, Aguirre E, et al. An accurate UTD extension to a ray launching algorithm for the analysis of complex indoor radio environments. *J Electromagnet Wave* 2016; 30(10): 43–60.
28. Komarov KK. *Handbook of dielectric and thermal properties of materials at microwave frequencies*. Boston, MA; London: Artech House, 2012.
29. Aguirre E, Arpón J, Azpilicueta L, et al. Evaluation of electromagnetic dosimetry of wireless systems in complex indoor scenarios within body human interaction. *Prog Electromagn Res B* 2012; 43: 189–209.
30. Led S, Azpilicueta L, Aguirre E, et al. Analysis and description of HOLTIN service provision for AECG monitoring in complex indoor environments. *Sensors* 2013; 13(4): 4947–4960.
31. Azpilicueta L, Rawat M, Rawat K, et al. Convergence analysis in deterministic 3D ray launching radio channel estimation in complex environments. *Appl Comput Electrom* 2014; 29(4): 256–271.
32. Banerjee SR, Jesme R and Sainati RA. Performance analysis of short range UHF propagation as applicable to passive RFID. In: *Proceedings of the IEEE international conference on RFID*, Grapevine, TX, 26–28 March 2007, pp.30–36. New York: IEEE.
33. Gomez C, Oller J and Paradells J. Overview and evaluation of bluetooth low energy: an emerging low-power wireless technology. *Sensors* 2012; 12: 11734–11753.
34. Pentaho Community 6, http://community.pentaho.com/
35. Open EMR, http://www.open-emr.org/
36. MySQL, https://www.mysql.com/
37. Symmetric DS, http://www.symmetricds.org/
38. Astrain JJ, Villadangos J, Garitagoitia JR, et al. Fuzzy location and tracking on wireless networks. In: *Proceedings of the 4th ACM international workshop on mobility management and wireless access*, Torremolinos, 2–6 October 2006, pp.84–91. New York: ACM.